Gradient-enhanced FAWSETS perfusion measurements

Kenneth I. Marro *, Donghoon Lee, Outi M. Hyyti

Department of Radiology, University of Washington, Seattle, WA 98195-7115, USA

Abstract

This work describes the use of custom-built gradients to enhance skeletal muscle perfusion measurements acquired with a previously described arterial spin labeling technique known as FAWSETS (flow-driven arterial water stimulation with elimination of tissue signal). Custom-built gradients provide active control of the static magnetic field gradient on which FAWSETS relies for labeling. This allows selective, 180° modulations of the phase of the perfusion component of the signal. Phase cycling can then be implemented to eliminate all extraneous components leaving a signal that exclusively reflects capillary-level perfusion. Gradient-enhancement substantially reduces acquisition time and eliminates the need to acquire an ischemic signal to quantify perfusion. This removes critical obstacles to application of FAWSETS in organs other than skeletal muscle and makes the measurements more desirable for clinical environments. The basic physical principles of gradient-enhancement are demonstrated in flow phantom experiments and in vivo utility is demonstrated in rat hind limb during stimulated exercise.
© 2005 Elsevier Inc. All rights reserved.

Keywords: Arterial spin labeling; Perfusion; Skeletal muscle; Custom-built gradient; FAWSETS

1. Introduction

The ^{1}H NMR-based techniques known as arterial spin labeling (ASL) are attractive to researchers and clinicians because they provide completely non-invasive, quantitative measurements of local capillary-level perfusion. ASL methods develop contrast and specificity by selectively perturbing (labeling) the spin state of coherently flowing arterial water. This transient label induces a change in the magnetization within the region of interest as the blood flows into the capillaries and diffuses into the tissue. Quantification can be achieved by measuring the effect of the label on either the tissue magnetization [1] or its T_1 relaxation rate [2]. Successful efforts have led to the development of more than a dozen variations of ASL techniques suitable for cerebral perfusion measurements, including pulsed labeling techniques and continuous, flow-driven adiabatic labeling schemes [3–5].

Our research group has previously developed an ASL technique—flow-driven arterial water stimulation with elimination of tissue signal (FAWSETS) [6]—that is particularly well suited for quantification of skeletal muscle perfusion because it eliminates magnetization transfer (MT) and arterial transit time effects [7,8]. These effects increase acquisition times and degrade accuracy of other ASL techniques and they are amplified by the unique physiological and hemodynamic properties of skeletal muscle.

FAWSETS as we have previously implemented it, which we will refer to here as basic FAWSETS, relies on gradients in both B_1 and B_0 to achieve flow-driven, adiabatic excitation of the arterial water as it flows into the sweet spot of the RF coil [6]. The B_1 gradient is determined by the geometry of the RF coil. The B_0 gradient occurs due to variations in the static magnetic field at the edges of the RF coil that arise during the shimming process. Convective flow of blood through these

---

* Corresponding author. Fax: +1 206 543 3495.
E-mail address: marro@u.washington.edu (K.I. Marro).

spatially variant B_1 and B_0 fields causes arterial water spins to experience time-dependent variations in the effective field, B_{eff} [9]. If adiabatic conditions are met for the range of relevant velocities the arterial water tips into the transverse plane as it flows into the sweet spot. While shim-generated B_0 gradients can result in consistent, effective (>90% in flow phantoms) excitation of in-flowing water [6], the fields are not optimized for flow-driven adiabatic manipulation and are not amenable to active control.

In the current work, we describe how custom-designed gradients can be implemented to provide active control over the required B_0 gradient. We show how manipulations in the B_0 gradient allow selective, 180° modulations of the phase of the in-flowing arterial water magnetization. Phase cycling can then be used to eliminate undesirable magnetization arising from partially saturated tissue water, leaving a signal that exclusively represents tissue perfusion. We present preliminary flow phantom and in vivo results that validate the basic principles of gradient-enhanced FAWSETS and we discuss other advantages including reduced acquisition times and removal of critical obstacles to application in organs other than skeletal muscle.

2. Results

We first present results showing that the prototype gradient produces the desired magnetic field and discuss how this allows active and selective modulation of the phase of the adiabatically excited arterial water magnetization. Our flow phantom results validate the basic principles in a simplified model. In vivo results from the rat hind limb demonstrate that gradient-enhancement allows phase cycling to filter out undesirable components leaving a signal that is directly proportional to local tissue perfusion.

Figs. 1 and 2 show the relevant magnetic fields as measured in a 1-cm diameter test tube filled with water. The upper panel in Fig. 1 shows the static field (ΔB_0) produced with positive 0.5 A flowing through our prototype gradient. The second panel shows the B_1 field produced by the saddle coil used in all these experiments and the third panel shows the approximate magnitude and angle of B_{eff} at discrete locations along the direction of arterial flow. The longitudinal component of B_{eff} is defined by ΔB_0 and the transverse component is equal to B_1 [9]. The bottom panel of both figures depicts the evolution of the arterial water magnetization as it flows into the sweet spot of the RF coil (see Section 3). Continuous labeling brings the net signal, M_f, within the sweet spot to a steady state consisting of a perfusion component, M_p, and a residual tissue component, M_{rt}, arising from incompletely saturated tissue water.

Fig. 2 shows the measured ΔB_0 and B_1 fields with negative 0.5 A flowing through the prototype gradient.
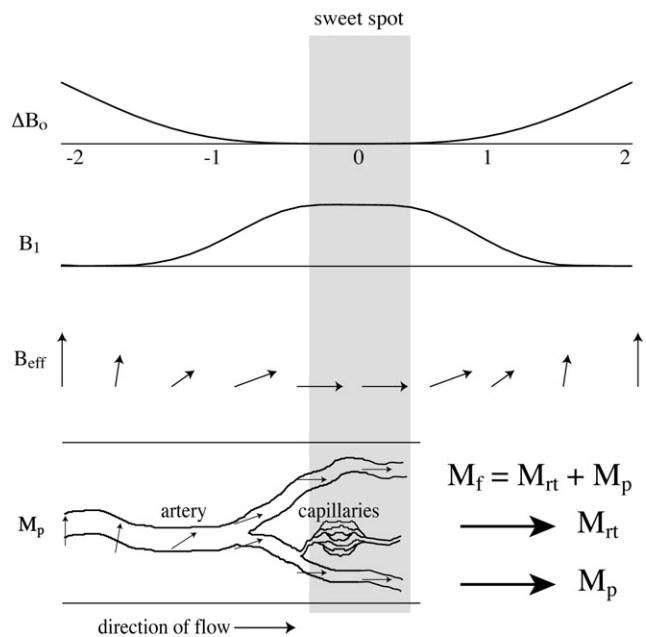

Fig. 1. The upper panel shows the measured ΔB_0 field produced by a positive 0.5 A current in our prototype gradient coil (dimensions along the abscissa are given in cm). The second panel shows the spatial variations in the B_1 field produced by our 2.5 cm long 2.5 cm diameter saddle coil. The ΔB_0 and B_1 fields shown were measured using a 1 cm diameter test tube filled with water. The third panel shows the approximate magnitude and angle of B_{eff} generated by ΔB_0 and B_1. At the left-most edge of the diagram, far from the sweet spot of the RF coil, there is a large and positive ΔB_0 and a zero B_1 so B_{eff} is purely longitudinal. Moving from left to right, toward the sweet spot of the RF coil, ΔB_0 decreases and B_1 increases so B_{eff} begins to tilt away from the longitudinal axis. Within the sweet spot ΔB_0 approaches zero and B_1 reaches a plateau so B_{eff} is purely transverse. The orientation of the magnetization arising from flowing water (M_p) is shown at several positions in the bottom panel of the diagram. At the left-most edge M_p is in its equilibrium position, which is purely longitudinal and aligned with B_{eff}. If adiabatic conditions are met throughout the process then M_p remains aligned with B_{eff} as it flows through these spatially changing magnetic fields. Within the sweet spot of the RF coil M_p is purely transverse and is parallel to both B_{eff} and the residual tissue signal (M_{rt}). The net signal, M_f, acquired from anywhere within the sweet spot is the sum of M_{rt} and M_p.

Reversing the flow of current in the coil inverts the shape of ΔB_0 and changes the orientation of B_{eff} outside the sweet spot of the RF coil. The fields within the sweet spot are unaffected by changes in current flow of this magnitude. By altering B_{eff} from the shape shown in Fig. 1 to that shown in Fig. 2 we were able to induce 180° modulations of the phase of the inflowing arterial water magnetization without altering the phase or amplitude of the magnetization arising from tissue water within the acquisition volume (see Section 3).

We tested the concept of gradient-enhanced FAWSETS using our prototype gradient and a simple flow phantom. The two spectra in Fig. 3 were acquired with water flowing through a 5 mm diameter tube centered axially in the probe with a positive 0.5 A current flowing in the gradient (solid line) and with a negative current of
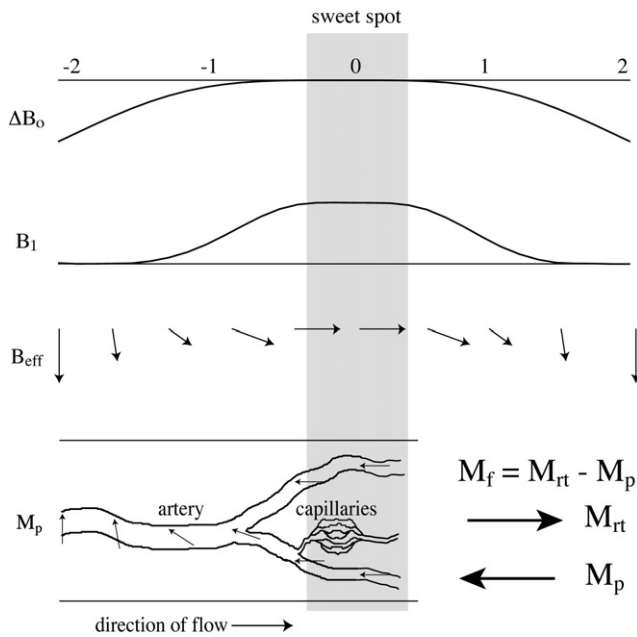
Fig. 2. When the current in the gradient coil is reversed the phase of M_p is selectively inverted 180°. The difference between this diagram and the previous one is that the sign of ΔB_0 is now negative. At the left-most edge of the diagram there is now a large negative ΔB_0 and zero B_1 so B_{eff} points straight down. As the water approaches the sweet spot B_{eff} begins to tip into the transverse plane. Within the sweet spot B_{eff} has the exact same orientation as it had in the previous diagram—it is purely transverse and points to the right—so the phase and amplitude of M_{rt} are unchanged. At the left-most edge M_p is in its equilibrium position, as in the previous diagram, but it is now antiparallel to B_{eff}. If adiabatic conditions are met throughout the process, M_p remains antiparallel to B_{eff} as it flows into the sweet spot. Within the sweet spot M_p is again purely transverse but now it is pointing to the left, opposite to B_{eff} and 180° out of phase relative to M_{rt}. The net signal acquired from anywhere within the sweet spot is now the difference between M_{rt} and M_p.
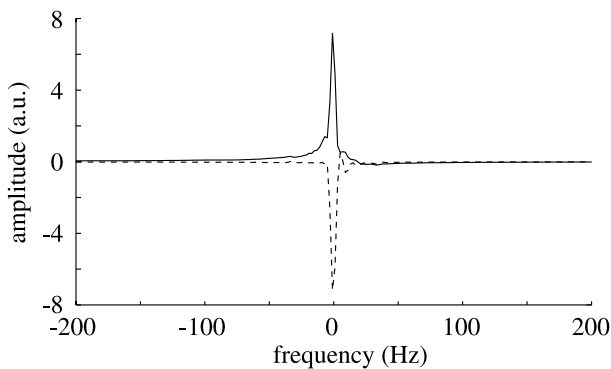

Fig. 3. Flow phantom spectra acquired using our saddle coil and prototype gradient. The flow phantom consisted of water flowing through a 5 mm inside diameter tube centered in the RF and gradient coils. The spectra were acquired from a 5 mm thick slice at the center of the RF coil following 5 s of FAWSETS excitation. The water peak in the spectrum acquired with a positive 0.5 A current flowing in the gradient coil (solid line) is 180° out of phase from the spectrum acquired with a negative 0.5 A current (dashed line).
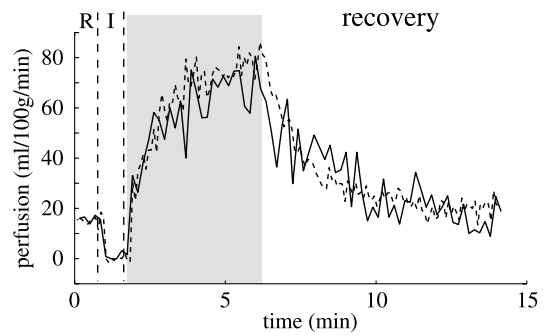

Fig. 4. In vivo gradient-enhanced FAWSETS results (solid line, $N = 6$) are in excellent agreement with basic FAWSETS results (dotted line, $N = 8$) acquired under the same conditions. Both data sets were acquired from a single voxel in the rat hind limb at rest (R), during ischemia (I), during stimulated exercise (shaded area), and during recovery. The gradient-enhanced FAWSETS results were processed without subtraction of the ischemic signal.

equal amplitude (dashed line). When the same phase correction factor was applied to both spectra the water peak was 180° out of phase. The behavior of the water magnetization in this example is analogous to the behavior of the magnetization of arterial water in vivo.

In vivo results (Fig. 4) demonstrate that gradient-enhanced FAWSETS allows phase cycling to eliminate M_{rt}. The data were acquired from the rat hind limb during stimulated exercise using gradient-enhanced FAWSETS (solid line) and basic FAWSETS (dashed line). Each data point for gradient-enhanced FAWSETS represents the subtraction of two signals acquired with opposite currents flowing in the gradient. Processing of the basic FAWSETS data included subtraction of an ischemic signal from all the data points. This was not necessary for the gradient-enhanced FAWSETS data, demonstrating that phase cycling completely eliminated M_{rt}, the residual tissue signal. The excellent agreement between the two data sets validates the basic physical principles described in Figs. 1 and 2. The S/N of the gradient-enhanced FAWSETS measurements is lower in these experiments because they were acquired from a smaller volume of tissue than the basic FAWSETS measurements. This could likely be improved by a more sophisticated RF/gradient probe design (see Section 3).

3. Discussion

Custom-built gradients enhance the FAWSETS labeling process by providing a higher degree of control over ΔB_0 than is allowed by the shim coils. The shape of the ΔB_0 field can be designed to optimize the flow-driven labeling process for the B_1 gradient produced by a particular RF coil. This could allow adiabatic conditions to be met with lower B_1 amplitude than is required for basic FAWSETS measurements. Custom gradients also allow active manipulation of ΔB_0, which can be exploited

to improve time resolution and utility compared to basic FAWSETS measurements.

The details of how FAWSETS works have been published previously [6]. The labeling process, which is similar to that of continuous arterial spin inversion [10–12], relies on appropriate spatial variations in B_{eff}. FAWSETS labeling occurs at the edges of the sweet spot of the RF coil, where there are gradients in both B_1 and B_0. The gradient in B_1 occurs because the RF field decreases as a function of distance away from the sweet spot of the coil. The gradients in B_0 arise from the shimming process. During the shim process the dominant signal comes from within the sweet spot of the RF coil and this defines the shimmed volume. Shimming yields a homogenous B_0 field within the shimmed volume but leaves a non-uniform field outside the shimmed volume. These spatially variant B_1 and B_0 fields are irrelevant in most MR measurements but they are critical to FAWSETS measurements, where they are exploited to generate flow-driven adiabatic excitation of arterial water as it flows into the sweet spot of the RF coil. Within the sweet spot, the arterial water magnetization remains spin-locked and relaxes according to $T_{1\rho}$ processes. After several seconds of continuous RF the basic FAWSETS signal reaches a steady state in which the area of the water peak consists of a freshly perfused water component, M_p, and a residual tissue component, M_{rt}, of approximately equal magnitude that arises from incompletely saturated tissue water.

The lower panels in Figs. 1 and 2 demonstrate schematically how reversing the flow of current in our custom gradient results in selective 180° phase modulations in the magnetization of inflowing arterial water. In Fig. 1, the magnetization of flowing water, M_p, is initially at equilibrium and is aligned parallel to B_{eff} at the left-most edge of the diagram. If adiabatic conditions are met M_p remains parallel to B_{eff} and tips into the transverse plane as it flows into the sweet spot of the RF coil. Within the sweet spot both ΔB_0 and B_1 are homogenous so M_p remains spin-locked and relaxes according to $T_{1\rho}$. The net signal, M_f, acquired after the system has reached steady state, is the sum of M_p and M_{rt}.

When the current in the gradient is reversed ΔB_0, and hence B_{eff}, get inverted (Fig. 2). The equilibrium orientation of M_p at the leftmost edge of the diagram is now antiparallel to B_{eff}. Flowing water still becomes adiabatically excited as it flows into the sweet spot but now it is 180° out of phase with respect to B_1. The phase and amplitude of M_{rt} are unaffected by current flow in the gradient because tissue water remains within the sweet spot at all times and experiences the same B_{eff}. The net signal now consists of the difference between M_p and M_{rt}. These two figures show schematically how gradient-enhancement allows selective modulation of the phase of M_p without altering the phase or amplitude

of M_{rt}. Selective phase modulation can be exploited through phase cycling to eliminate M_{rt}, leaving a signal that exclusively represents capillary-level perfusion.

Custom gradients can alleviate the following limitations to basic FAWSETS:

- Basic FAWSETS labeling must be continuous for about 5 s for both components (M_p and M_{rt}) of the signal to reach steady state. Signal-to-noise is maximized if the labeling period is long enough for M_p to reach a steady state. This requires about five times $T_{1\rho}$, or about 500 ms under the conditions of our basic FAWSETS measurements in rat hind limb at 4.7 T. It is not necessary for M_{rt} to reach a steady state but its amplitude must be consistent throughout a series of measurements if the same ischemic signal is to be subtracted from all the measurements. Consistency is assured if the labeling period is long enough for M_{rt} to also reach a steady state but this requires five times the T_1 of tissue at 4.7 T, or about 5 s.
- An ischemic signal is required to identify and eliminate M_{rt}. The RF power required to completely saturate the tissue signal could approach or exceed SAR limits set by the FDA. Because of safety concerns, in vivo basic FAWSETS signals contain contributions from both M_p and M_{rt}. We previously removed M_{rt} by subtracting an ischemic signal acquired with a blood pressure cuff inflated so that it contains only M_{rt}. Ischemia is not well tolerated in severe disease states or trauma conditions where limb blood flow is compromised. It is also extremely difficult and traumatic to induce ischemia in organs other than limb skeletal muscle.
- Relatively high SAR is required to assure high labeling efficiency. Since shim-generated B_0 gradients are not optimized for flow-driven adiabatic excitation, the labeling process requires relatively high RF amplitude, which leads to high SAR. It is safe to perform basic FAWSETS experiments in human limbs, where the FDA limits are 12 W/kg, but the limits for body and head are lower.

Our flow phantom results (Fig. 3) demonstrate that inversion of M_p can be achieved using a relatively simple gradient design. If the current flow is reversed in successive acquisitions, phase cycling techniques can be employed to eliminate M_{rt} and enhance M_p. Since M_{rt} can be eliminated it is no longer necessary to wait five times the tissue water T_1 for it to reach steady state. This allows the labeling period to be reduced to about five times $T_{1\rho}$ of arterial water, long enough for M_p to reach steady state. A two-step phase cycling scheme is required so the net acquisition time is reduced by a factor of $T_1/2T_{1\rho}$, or about five under the conditions of our in vivo measurements. Sensitivity to perfusion is also improved since signal averaging provides a $\sqrt{2}$ increase in S/N. We

were not able to test the limits of time resolution in these experiments because our prototype system required manual switching to control the flow of current in the gradient. The shortest labeling period we could practically implement was 1 s. Full implementation of gradient-enhanced phase cycling will require minor software modifications and a gradient power supply that can be controlled by the pulse sequence. The actual reduction in acquisition time will depend on the field strength and other experimental conditions.

Gradient-enhancement also eliminates the need to acquire an ischemic signal to remove M_{rt}. This will allow quantitative measurements to be conducted in skeletal muscle of severely diseased patients and will remove a critical obstacle to potential application in other organs.

Custom-built gradients could potentially allow a reduction in the amplitude of B_1 needed during the labeling period and thereby remove another obstacle to application in organs other than skeletal muscle. During the labeling process the adiabaticity factor depends on the shape amplitude of the B_1 and B_0 gradients and on the arterial flow velocity [13–15]. Shim-generated B_0 gradients are not optimized for labeling and relatively high B_1 amplitudes are required to ensure that adiabatic conditions are met over a wide range of arterial flow velocities. Gradient-enhancement could allow optimization of ΔB_0 for the B_1 field produced by a particular RF coil so that adiabatic conditions can be maintained along the direction of flow with lower B_1 amplitude than is required for basic FAWSETS measurements. This would reduce the possibility of tissue heating. Further tests are required to determine how much B_1 may be reduced by gradient-enhancement.

An important requirement for gradient-enhanced FAWSETS is that the field produced by the custom gradients must dominate ΔB_0 at the edges of the sweet spot of the RF coil, where the adiabatic excitation process occurs. The shape of ΔB_0 depends not only on the field produced by the custom gradients but also on the sample shape, geometry, and composition and on the currents flowing in the shim coils. If significant non-uniformities exist at the edges of the sweet spot, the shape of ΔB_0 will not be symmetric when the current in the custom gradients is reversed. Significant asymmetry in ΔB_0 could impede the phase modulation of M_p and/or affect its amplitude. We addressed this issue by implementing a two-step shimming process (see Section 5) intended to extend the homogenous B_0 field beyond the sweet spot of the RF coil into the regions where the B_1 gradients occur in Figs. 1 and 2. In the current experiments, the animals were all approximately the same size and the two-step shimming process appears to have worked adequately. It is difficult to predict how much shim currents could degrade the measurements in more routine experiments, where the sample could vary considerably more than in these preliminary experiments. In some cases it may be necessary to shim with a larger RF coil than the one used for the perfusion measurements.

In the current experiments the S/N for gradient-enhanced FAWSETS appears to be lower than for basic FAWSETS (Fig. 4). There are two explanations for this. First, the gradient-enhanced FAWSETS measurements were acquired from a volume of tissue about 50% smaller than the basic FAWSETS measurements. This was because the prototype gradient prevented the rats' hind limbs from being pulled as far into the RF coil and forced the acquisition volume to be located more toward the ankle region, where there is less muscle tissue. Second, neither the RF coil nor the custom gradient were fabricated to high tolerances. Our goal was simply to demonstrate proof of concept so simplicity was an important constraint imposed on the design. Both coils were built using readily available components and processes. A more sophisticated RF/gradient probe design, implementing machined components and etched circuitry, could allow proper positioning of the hind limb and would provide improved alignment and symmetry. This would likely result in more consistent excitation of the arterial water.

While gradient-enhancement offers several improvements over basic FAWSETS, the question of how well it compares to other more established ASL techniques remains. Our previous work [8] demonstrated that FAWSETS eliminates MT effects and this could be an important consideration in applications where the effects are expected to be large and change rapidly. The FAWSETS label is applied as the arterial water flows into the acquisition volume. This offers advantages in terms of sensitivity but is at least partially offset by the fact that the label subsequently decays according to $T_{1\rho}$. With other ASL techniques the decay of the label is governed by T_1, which is considerably longer. FAWSETS reduces sensitivity to transit times by eliminating the time required for the arterial water to flow from the labeling plane to the acquisition plane but it does not eliminate the time required for the labeled water to flow from larger arteries to the capillary beds within the acquisition plane. Our previous FAWSETS measurements in rat hind limb were in good agreement with similar measurements made with microspheres despite the fact that we ignored the transit time. In other applications, where the vascular geometry is larger, it may be necessary to compensate for these effects. Another consideration is that the sensitivity of the FAWSETS label (excitation of the arterial water) is inherently a factor of 2 lower than ASL techniques that use inversion as the label.

These points are important to consider when weighing the benefits of FAWSETS against other ASL techniques. The choice of the optimum technique for a particular application is likely to depend on a number of factors. Some of these—such as the vascular geome-

try of the organ involved, the RF coil geometry, the expected MT effects, the applicable SAR limitations, the B_0 field strength and the relevant relaxation times—are known or can be easily measured. Others—such as the transit time, the range of arterial flow velocities and the capillary/tissue exchange time for water—may be difficult to estimate.

4. Conclusions

This preliminary work demonstrates that time resolution and utility of FAWSETS perfusion measurements can be substantially improved through the use of custom-built gradients. Our relatively simple gradient design allowed us to actively control the static magnetic fields at the edges of the RF coil where the flow-driven adiabatic excitation process, on which FAWSETS depends for labeling, takes place. Our flow phantom experiments demonstrate the key principle of gradient-enhanced FAWSETS: the phase of the signal from in-flowing arterial water can be selectively modulated by reversing the flow of current in the custom gradient. Phase cycling can then be implemented to yield a signal arising exclusively from freshly perfused arterial water. Our in vivo results demonstrate the main advantages of gradient-enhance FAWSETS over basic FAWSETS: substantial improvement in time resolution and elimination of the requirement to acquire ischemic measurements. This makes the measurements more appropriate for clinical environments and removes critical barriers to implementation in organs other than skeletal muscle.

5. Experimental

Flow phantom measurements were conducted to demonstrate the physical principles of gradient-enhanced FAWSETS. In vivo measurements were conducted to test feasibility and demonstrate potential improvements in rat hind limb muscle. Both sets of experiments were conducted in a 4.7 T horizontal bore Bruker magnet controlled by a Varian Inova console running VNMR version 6.1.

5.1. Prototype gradient design and field measurements

The first step in the gradient design process was to measure the shape of the B_1 field produce by the RF coil used in the rat hind limb measurements, which was a 2.5 cm diameter, 2.5 cm long saddle coil tuned to the water resonance (200.1 MHz). This was accomplished by acquiring a z-axis profile from a 1 cm diameter test tube filled with water and centered in the coil. The B_1 field shape was then used as an input to a software tool we have developed to model flow-driven adiabatic
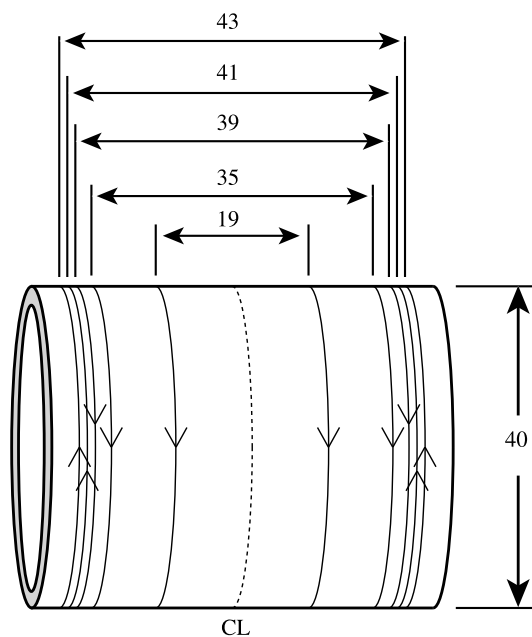

Fig. 5. A schematic of the prototype gradient coil implemented in both the flow phantom and in vivo measurements. The gradient was designed so that a 2.5 cm diameter by 2.5 cm long RF coil, including the tune and match capacitors, could fit inside it. The circuit consists of 10 conducting loops with relative current directions shown by the arrowheads. Spacing of the current loops is symmetric about the center-line (CL) of the gradient. Dimensions are given in millimeters.

manipulations [15]. The model assumed a laminar flow velocity of 30 cm/s—the maximum velocity of blood flow expected in the rat femoral artery [16]—and generated a target ΔB_0 field that would satisfy adiabatic conditions [9] for all points along the z-axis, the direction of flow in both the flow phantom and in vivo experiments. The target field method [17–19] was then used to determine the number and location of current loops needed to produce the target ΔB_0 field with the additional constraint that the diameter of the gradient be large enough to accommodate the RF coil. A diagram of the resulting gradient geometry is provided in Fig. 5.

A simple, manually switched current-controlled power supply was used to drive the gradient circuit. To measure the ΔB_0 field it produced (Figs. 1 and 2), a 1 cm diameter test tube filled with water was placed in the combined RF/gradient probe. The current in the gradient was maintained at plus or minus 0.5 A throughout the measurements. A series of z-axis profiles were acquired (using the standard z-axis gradient of the scanner) following a hard 90° pulse with the delay time between signal excitation and acquisition incremented from 10 to 200 ms in 5 ms increments. The subsequent 2-D Fourier transform yielded frequency as a function of position.

5.2. Shimming

An important requirement for gradient-enhanced FAWSETS is that ΔB_0 must be symmetric when the cur-

rent in the custom gradient is reversed. That is, the two ΔB_0 fields shown in Figs. 1 and 2 must appear to be mirror images of each other. This requirement can be met if the B_0 homogeneity (with no current flowing in the custom gradient) extends beyond the sweet spot of the RF coil to include the regions where the B_1 gradients occur. To accomplish this, shimming was conducted in two stages. First, the B_1 power and pulse width were set to yield a hard 180° pulse within the sweet spot of the RF coil. This ensured that the dominant signal came from the regions just outside the sweet spot. The higher order shim currents were then adjusted to optimize B_0 field homogeneity. The B_1 power and pulse width were then reset to yield a hard pulse with a flip angle of approximately 30° within the sweet spot and the three linear shim currents were adjusted with the dominant signal arising from within the sweet spot. Both stages of the shimming process were conducted with no current flowing in the custom gradient.

5.3. Flow phantom measurements

Flow phantom measurements were conducted to test whether control of the shape of ΔB_0 would allow the phase of adiabatically excited water flowing into the RF coil to be inverted. The flow phantom consisted of water flowing through a 5 mm inside diameter tube centered in the RF and gradient coils. FAWSETS measurements were acquired with the average flow velocity in the tube set to about 10 cm/s, as determined by timed collection of the outflow. The FAWSETS pulse sequence has previously been described in detail [6]. Briefly, signal excitation consisted of continuous RF at about 50 mG for 4 s in the absence of gradients. This was followed by a 180°, 5 mm thick axial slice-select pulse (4 ms duration) to localize the signal in the center of the RF coil. Data were acquired as free induction decays (FID's) with 4000 Hz sweep width, 1000 complex points and signal averaging set to four. FID's were acquired with both positive 0.5 A and negative 0.5 A flowing through the gradient circuit.

5.4. Rat hind limb measurements

To demonstrate feasibility of in vivo measurements both basic FAWSETS and gradient-enhanced FAWSETS measurements were acquired from rat hind limb muscle at rest, during ischemia, during stimulated exercise and during recovery. All animal procedures were in accordance with guidelines of the University of Washington Animal Care Committee and the National Institutes of Health. Male Sprague–Dawley rats weighing 280–320 g were anesthetized with isoflurane inhalation throughout the entire experiment. Stimulated contractions of all hind limb muscles were induced via an electrode placed around the exposed sciatic nerve using a previously described protocol [8]. To avoid degradation of the perfusion measure-

ments due to motion artifacts the stimulation protocol consisted of short (250 ms) tetanic contractions every 5 s. This provided a sufficiently long quiescent period between contractions to easily accommodate signal acquisition following the 4 s of continuous spin labeling needed for the basic FAWSETS measurements. The contractile force generated during each contraction was actively maintained at 40% of the maximum stimulated contraction (MSC), or the maximum contractile force that could be generated by that animal.

Immediately after surgery the right hind limb was extended (using a suture inserted through the ankle) and secured into the RF/gradient probe. The probe was centered in the bore of the magnet and shimming was conducted using the procedure described above.

For comparison purposes both basic FAWSETS (eight animals) and gradient-enhanced FAWSETS (six animals) measurements were acquired. The labeling protocol for the basic FAWSETS measurements consisted of 4 s of continuous on-resonance RF with amplitude of about 120 mG. This was followed by a slice-selective 180° pulse to localize the signal from a 5 mm thick slice located at the proximal edge of the sweet spot of the RF coil. Location of the slice was facilitated by a z-axis profile and was approximately at the midpoint between the knee and ankle. The hind limb diameter at this location is about 1.8 cm so the acquisition volume was approximately 1.25 ml.

The labeling protocol for the gradient-enhanced FAWSETS measurements was the same as for the basic FAWSETS measurements except that current flow in the custom-built gradient alternated between positive and negative 0.5 A in successive acquisitions. Even numbered acquisitions (acquired with positive current flowing in the gradient) were subtracted from the previous odd numbered acquisitions (acquired with negative current flowing in the gradient).

Symmetric crusher gradients ($b = 5$ s/mm^2, 2.5 G/cm, 4 ms duration, and 8.5 ms separation) around the slice-select pulse were used to attenuate signal outside the slice and to filter out signal from faster flowing arterial water [20]. Data were acquired as FID's during the second half of the spin echo generated by the 180° pulse. Acquisition parameters included 4000 Hz sweep width, 1000 complex points, echo time (TE) = 14.0 ms, and no signal averaging. Repetition time (TR) was set to 5 s and, during stimulation periods, was gated by the stimulation pulse generator so that signal excitation and acquisition were interleaved between muscle contractions. The RF transmitter frequency was reset to the water resonance after every 10 acquisitions.

5.5. Data analysis

Spectral analysis was performed using the Advanced Method for Accurate, Robust and Efficient Spectral fit-

ting (AMARES) time domain fitting algorithm [21] as included in the Java-based Magnetic Resonance User Interface (jMRUI) software package [22]. Perfusion quantification was achieved using a model developed to quantify perfusion with continuous arterial spin inversion [10], but modified to account for the conditions of FAWSETS excitation

$$f = \frac{\lambda}{\alpha T_{1\rho}} \frac{M_f - M_{rt}}{M_0},$$ (1)

where f is perfusion in ml/g/min, λ is the tissue/blood partition coefficient, which was assumed to be 0.7 ml/g [23], α is the labeling efficiency, which was assumed to be 0.9 based on previous measurements conducted in flow phantoms [6], $T_{1\rho}$ is the relevant relaxation constant for spin-locked arterial water during the labeling period, M_f is the steady state FAWSETS signal following continuous labeling, M_{rt} is the residual, steady state tissue signal acquired after continuous labeling with blood flow occluded and M_0 is the equilibrium magnetization. The modification to the original model consisted of replacement of T_1 with $T_{1\rho}$. The justification for use of this model and the modification is that the physical principles governing the behavior of the labeled arterial water are the same in a FAWSETS experiment as in continuous arterial spin inversion except that the labeled arterial water relaxes according to $T_{1\rho}$ instead of T_1. Measurements conducted on oxygenated rat blood showed $T_{1\rho}$ to be 110 ms at the B_1 magnitude used for labeling (about 120 mG).

Acknowledgments

References

[1] J.A. Detre, J.S. Leigh, D.S. Williams, A.P. Koretsky, Perfusion imaging, Magn. Reson. Med. 23 (1992) 37–45.

[2] K.K. Kwong, J.W. Belliveau, D.A. Chesler, I.E. Goldberg, R.M. Weisskoff, B.P. Poncelet, D.N. Kennedy, B.E. Hoppel, M.S. Cohen, R. Turner, H. Cheng, T.J. Brady, B.R. Rosen, Dynamic magnetic resonance imaging of human brain activity during primary sensory stimulation, Proc. Natl. Acad. Sci. USA 89 (1992) 5675–5679.

[3] E.L. Barbier, L. Lamalle, M. Decorps, Methodology of brain perfusion imaging, J. Magn. Reson. Imaging 13 (2001) 496–520.

[4] F. Calamante, D.L. Thomas, G.S. Pell, J. Wiersma, R. Turner, Measuring cerebral blood flow using magnetic resonance imaging techniques, J. Cereb. Blood Flow Metab. 19 (1999) 701–735.

[5] X. Golay, J. Hendrikse, T.C. Lim, Perfusion imaging using arterial spin labeling, Top. Magn. Reson. Imaging 15 (2004) 10–27.

[6] K. Marro, FAWSETS: flow-driven arterial water stimulation with elimination of tissue signal, J. Magn. Reson. 124 (1997) 240–244.

[7] K.I. Marro, O.M. Hyyti, M.A. Vincent, M.J. Kushmerick, Validation and advantages of FAWSETS perfusion measurements in skeletal muscle, NMR Biomed. (2005) (in press).

[8] K.I. Marro, O.M. Hyyti, M.J. Kushmerick, FAWSETS perfusion measurements in exercising skeletal muscle, NMR Biomed. (2005) (in press).

[9] M. Garwood, L. DelaBarre, The return of the frequency sweep: designing adiabatic pulses for contemporary NMR, J. Magn. Reson. 153 (2001) 155–177.

[10] D.S. Williams, J.A. Detre, J.S. Leigh, A.P. Koretsky, Magnetic resonance imaging of perfusion using spin inversion of arterial water, Proc. Natl. Acad. Sci. USA 89 (1992) 212–216.

[11] W. Zhang, D.S. Williams, A.P. Koretsky, Measurement of rat brain perfusion by NMR using spin labeling of arterial water: in vivo determination of the degree of spin labeling, Magn. Reson. Med. 29 (1993) 416–421.

[12] J.A. Detre, D.C. Alsop, Perfusion magnetic resonance imaging with continuous arterial spin labeling: methods and clinical applications in the central nervous system, Eur. J. Radiol. 30 (1999) 115–124.

[13] J.F. Utting, D.L. Thomas, D.G. Gadian, R.J. Ordidge, Velocity-driven adiabatic fast passage for arterial spin labeling: results from a computer model, Magn. Reson. Med. 49 (2003) 398–401.

[14] L. Maccotta, J.A. Detre, D.C. Alsop, The efficiency of adiabatic inversion for perfusion imaging by arterial spin labeling, NMR Biomed. 10 (1997) 216–221.

[15] K.I. Marro, C.E. Hayes, M.J. Kushmerick, A model of the inversion process in an arterial inversion experiment, NMR Biomed. 10 (1997) 324–332.

[16] D. Dawson, M.A. Vincent, E.J. Barrett, S. Kaul, A. Clark, H. Leong-Poi, J.R. Lindner, Vascular recruitment in skeletal muscle during exercise and hyperinsulinemia assessed by contrast ultrasound, Am. J. Physiol. Endocrinol. Metab. 282 (2002) E714–E720.

[17] R. Turner, Gradient coil design: a review of methods, Magn. Reson. Imaging 11 (1993) 903–920.

[18] R. Turner, A target field approach to optimal coil design, J. Phys. D 19 (1986) L147–L151.

[19] R. Turner, Minimum inductance coils, J. Phys. E 21 (1988) 948–952.

[20] F.Q. Ye, V.S. Mattay, P. Jezzard, J.A. Frank, D.R. Weinberger, A.C. McLaughlin, Correction for vascular artifacts in cerebral blood flow values measured by using arterial spin tagging techniques, Magn. Reson. Med. 37 (1997) 226–235.

[21] L. Vanhamme, A. van den Boogaart, S. Van Huffel, Improved method for accurate and efficient quantification of MRS data with use of prior knowledge, J. Magn. Reson. 129 (1997) 35–43.

[22] A. Naressi, C. Couturier, J.M. Devos, M. Janssen, C. Mangeat, R. de Beer, D. Graveron-Demilly, Java-based graphical user interface for the MRUI quantitation package, Magma 12 (2001) 141–152.

[23] G. Radegran, Limb and skeletal muscle blood flow measurements at rest and during exercise in human subjects, Proc. Nutr. Soc. 58 (1999) 887–898.